metals

MDPI

Article

Impact of Copper, Tin and Titanium Addition on Bending-Induced Damage of Intermetallic Phases in Hot Dip Galvanizing

Costanzo Bellini *, Vittorio Di Cocco, Francesco Iacoviello and Larisa Patricia Mocanu

Department of Civil and Mechanical Engineering, University of Cassino and Southern Lazio, Via G. Di Biasio, 43, 03043 Cassino, FR, Italy
* Correspondence: costanzo.bellini@unicas.it

Abstract: Hot dip galvanizing is among the cheapest methods for protecting ferrous alloys against corrosion. The success is due to both the low cost of the process and the high degree of protection in many corrosive environments, where the coatings serve as sacrificial protection. The purpose of this analysis is to study the mechanical characteristics of steel plates, that have been hot dip coated with five different zinc alloy molten bath for different time periods. The mechanical tests performed is a non-standardized four-point bending test considering three distinct bending angles. Results are examined in terms of both mechanical behaviour and coating phase damage. The development of intermetallic phases and their damage are both influenced by the chemical compositions of the zinc bath, demonstrating that fractures arise mostly at the substrate-coating interface. All the coatings showed the arising of micro-cracks except for the Aluminium, which demonstrated its ductility. In addition, Zn-Ti coatings showed the arising of a new compact phase rich in iron, characterized by a great hardness. More research is needed to explore the aluminium impact on the zinc bath, the lack of tiny fractures in the phase, and the lesser thickness compared to the other coatings tested.

Keywords: damage; hot dip galvanizing; bath chemical composition; intermetallic phases; four-points bending test; microstructure; hypersandelin steel

Citation: Bellini, C.; Di Cocco, V.; Iacoviello, F.; Mocanu, L.P. Impact of Copper, Tin and Titanium Addition on Bending-Induced Damage of Intermetallic Phases in Hot Dip Galvanizing. *Metals* **2022**, *12*, 2035. https://doi.org/10.3390/met12122035

Academic Editor: Frank Czerwinski

Received: 31 October 2022
Accepted: 23 November 2022
Published: 26 November 2022

1. Introduction

Today, hot dip galvanizing (which consists of applying a metallic zinc coating to steels from a batch of molten metal) is widely among the most employed solution for protection against the corrosion of steel. Its success is due to the high and effective protection it provides to metal parts operating in a wide variety of aggressive environments; moreover, it is an economical process, easy to be performed [1]. The high corrosion resistance is given by two peculiar characteristics of hot dip galvanizing:

- a barrier effect that physically separates the metal material from the aggressive environment; [2]
- a galvanic protection effect due to the difference in the electrochemical potentials between the zinc coating and the steel substrate, being the electrochemical potential of the former lower than that of the latter [3–5].

Moreover, the abovementioned characteristics are enhanced by the high adhesion of the zinc layer to the metallic substrate. Due to the interdiffusion phenomena of iron and zinc atoms, that happen on the part surface, the coatings are characterized by zones of different chemical compositions [6–9]. The layers closer to the metallic substrate are characterized by a higher iron content; on the contrary, the external areas present a chemical composition analogous to that of the galvanizing bath (essentially, zinc with little iron content due to the transfer of iron atoms from galvanizing previously carried out in the bath). As visible in Figure 1, the difference in chemical composition determines the occurrence of four different intermetallic phases [1]:

- The phase in contact with the substrate to be protected is the Γ phase, which includes all the phases with an iron content between 17% and 28% by weight. It is characterized by a high degree of brittleness and its depth can be occasionally neglected in comparison to the depths of the other ones.
- The phase immediately external to phase Γ is phase δ, which presents an iron quantity between 7% and 11.5% by weight. It has a compact morphology, it is characterized by a brittle mechanical behaviour and by a hardness higher than that of the steel used as a support to be protected, which generally consists of low carbon steels.
- The phase in contact with the δ phase is the ζ phase and is characterized by an iron amount between 5% and 6% by weight. Usually, its morphology is columnar due to its growth by directional diffusion in the solid phase of iron atoms from the δ phase and zinc atoms from the molten bath. With prolonged stays at high temperatures (e.g., in 460 °C baths for periods of more than 6 min), it can collapse into an undirected microstructure.
- The η phase is present in the outermost part of the coating and, therefore, constitutes its surface. The iron content of this phase is very low; in fact, its chemical composition is comparable with that of the galvanizing bath because it is generated by the solidification of the molten zinc layer obtained by wettability during extraction from the bath. Compared to the other intermetallic phases, its hardness is quite low and its toughness is higher due to the reduced iron content.

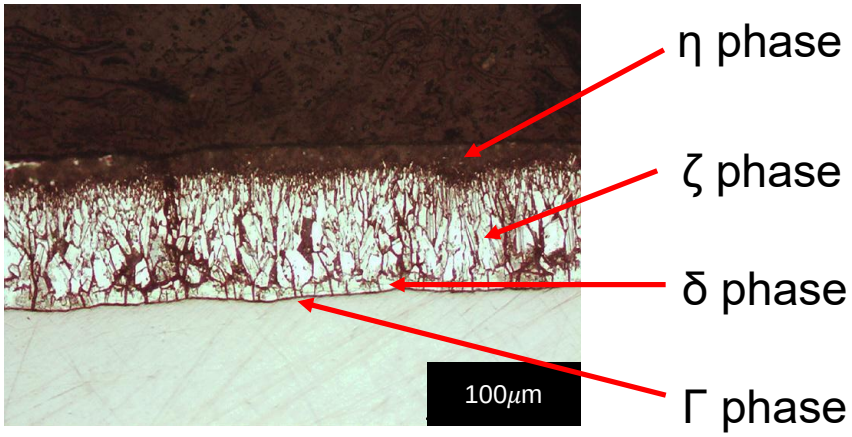

Figure 1. Hot dip galvanized coatings: typical intermetallic phases.

The described phases characterize the galvanic layers given by pure zinc baths, but often, in the production industrial realities, different alloying elements are added to the galvanizing bath to improve the wettability and the fluidity [10–12]. More recent research has found that alloying elements, such as 10% aluminium, also increase corrosion resistance, most likely due to the creation of a very stable and protective corrosion product phase known as simonkolleite [13]. Both the speed of intermetallic phase growth and the characteristics of the phases can be altered by alloying elements. The alloying elements that are not able to modify the characteristics of the intermetallic phases typical of pure zinc bath coatings are generally added to improve the diffusion phenomena and the wettability of the bath. In the past, the main element used to improve hot dip galvanizing was lead, which ensured more robust production processes capable of generating coatings with fewer defects. This element acts on the formation of the external phase η which constitutes the surface of the coating [14–16]. However, today lead has been eliminated from the baths as it is dangerous for human health, and the research has been oriented towards the identification of one or more elements capable of optimizing the hot dip galvanizing processes. Currently, the alloying element added in the baths that has replaced lead in most of the production realities is tin.

However, also alloying elements affecting the interdiffusion phenomena between Fe and Zn, like aluminium and titanium, have been investigated. The coatings obtained from these baths do not have the traditional intermetallic phases. Moreover, these coatings can influence the mechanical behaviour of the metal itself. In fact, it is known that galvanising can change the mechanical properties of parts, as demonstrated in the literature [17–19].

The goal of this work is to investigate the impact that specific alloying metals added in the zinc bath have on the kinetics of intermetallic phase development. To this aim, various immersion periods have been considered. The obtained coatings have been subjected to four-point bending tests to verify the influence of the coating on the mechanical behaviour. The sections of the deformed specimens have been analysed with the metallographic light optical microscope (LOM) in order to verify the damage of the intermetallic phases at three different angular deformation values. A damage parameter, assumed as the number of cracks per millimetre of deformed arc, has been used to quantify the damage values.

2. Materials and Methods

In this research work, a commercial hypersandelin steel provided by a local supplier was used as a coating steel. Table 1 lists the amount of alloying elements. The samples were produced by cutting them from a 3-mm-thick hot-rolled steel plate. The cut-out samples to be coated have dimensions of 80 × 25 mm.

Table 1. Amount of alloying elements of analyzed galvanized plates.

wt% C	wt% Si	wt% Mn	wt% P	wt% S	wt% N
0.090	0.167	0.540	0.010	0.004	—

The samples underwent pre-galvanizing preparatory work by being submerged at first in a surfactant-containing solution and then in an acid bath made from diluted hydrochloric acid at room temperature. These two steps were necessary to remove greasy impurities and iron oxides, respectively, that were present on the surface resulting from corrosion phenomena. In order to achieve a thin surface layer that is suitable to protect the substrate steel during galvanizing, the specimens to be processed were finally submerged in a 500 g/L solution of double salt of zinc chloride and ammonium chloride. This is done because the sublimation of the salt, during hot dip galvanization, creates an atmosphere based on strongly reducing ammoniacal fumes close to the steel-zinc bath contact. Five different bath compositions were taken into consideration in this study:

- Pure zinc,
- Zinc with 3% by weight of tin,
- Zinc with 0.5% by weight of copper,
- Zinc with 0.5% by weight of titanium,
- Zinc with 5% by weight of aluminium.

The 5% aluminium concentration was chosen not only to improve the molten bath and reduce the growth of brittle Fe-Zn intermetallic layers at the steel coating interface [20], but also to have a higher corrosion resistance, as is well reported in the literature where the inhibition layer thickness increases with Aluminium concentration in zinc bath [21]. The other percentages were chosen based on this proportion of Al to have a comparable effect with the same electrical reactivity.

Following a day of homogenization at 480 °C, all of the baths were utilized before being reduced to 460 °C for galvanizing. After that, three specimens were immersed in zinc for periods of 15, 60, 180, 360, and 900 s in order to study the precise kinetics of coating creation. Specimens were then tested on the 100 kN Galdabini Sun 10 (Galdabini Cesare S.p.A., Cardano al Campo, VA, Italy) universal testing machine utilizing a non-standard device that allows for four-point bending tests, Figure 2. To provide an elastic recovery angle of 30, 20, and 10 degrees on each head, three alternative bending angles were examined; therefore, a total of 60, 40 and 20 degrees of residual total deformation

angle between the two clamping zones were considered, respectively. A bending angle of 30 degrees corresponds to a crosshead displacement of 35 mm, as shown in Figure 2c.

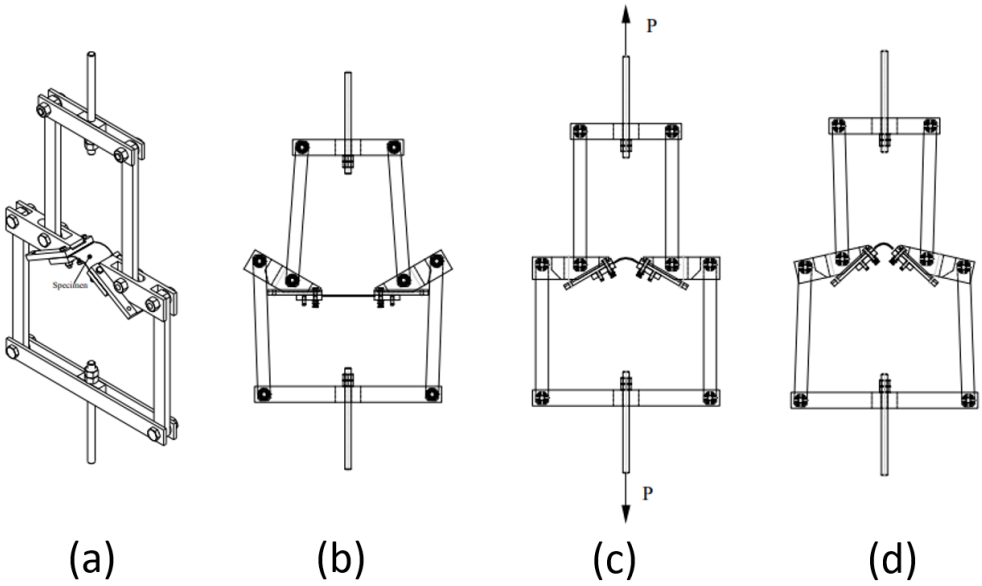

Figure 2. (**a**) clamping system for bending test. Different clamping configurations (**b**) Starting position; (**c**) Pure applied bending moment corresponding to 30°; (**d**) generic position [22].

Standard metallographic preparatory work, enabled Light Optical Microscope (LOM) analysis on the coating section on the tensile side of specimens. More in detail, sections of samples were mounted in phenol-formaldehyde resin using a Struers LaboPress-1 (Struers LLC, Cleveland, OH, United States) hot mounting press, producing cylindrical molds that facilitated handling of the specimens for grinding/polishing procedures. Each mounted specimen was ground using SiC paper with increasing mesh size of #240, 400, 600, 800, 1000, and #1200. Mirror finish polishing was performed on porous woven wool felt using a 1 µm and 0.3 µm Alumina suspension employing the standard polishing method. After the polishing procedures were completed, the samples were etched by immersion in Nital 2 for 15 s and then washed with ethanol. The intermetallic phases contained in the coating and the verification of the presence of cracks and their growth were analyzed with the Nikon Epithot (Nikon Corporation, Tokyo, Japan) inverted Metallurgical Microscope. The number of radial cracks per length of the deformed arc has been evaluated as a damage metric. Even if not all the damages can be quantified by using this parameter, since longitudinal and intergranular cracks are hardly observed, it was considered for this work since radial cracks are the main damage which characterizes the failure of the tensile zone in bending tests.

3. Results

Coatings obtained from a zinc plating bath containing only zinc were used in order to compare the effects of the other alloying elements. Figure 3 shows the results obtained from the bending tests of this type of specimen. The differences in the highest values of the measured bending moment are due to the thickness of the coatings. In general, the highest values are relevant to longer immersion times because they generate coatings with a greater thickness.

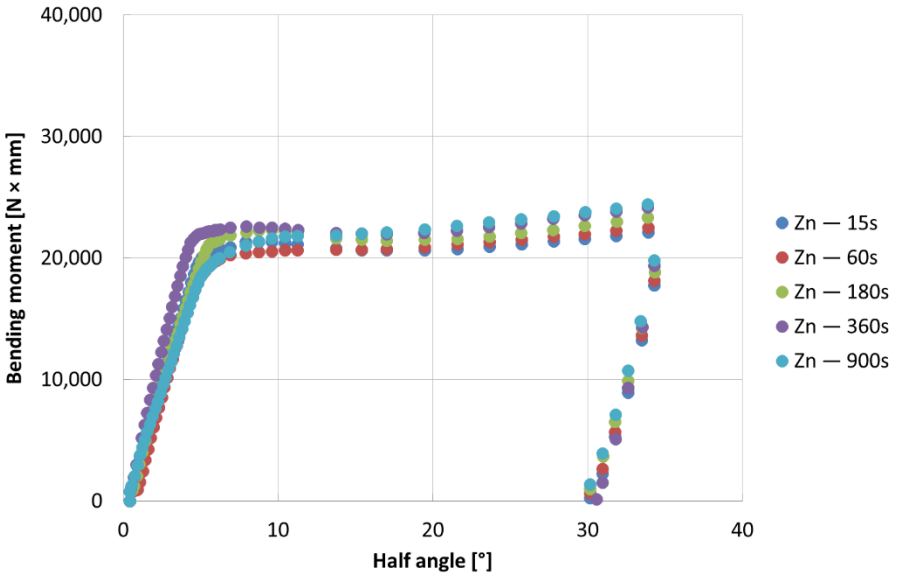

Figure 3. Bending tests results for specimens from pure Zn bath.

Figure 4 shows the angle-moment curves of the bending tests performed on the coating obtained from the baths containing tin and copper. The results confirm that the maximum flexural strength is obtained for specimens characterized by the maximum immersion times in the bath, corresponding to the maximum thicknesses of the coatings. Furthermore, the results obtained for the specimens containing tin show the maximum resistance values. Tin is currently the most widely used element as a substitute for the lead for the optimization of galvanizing baths.

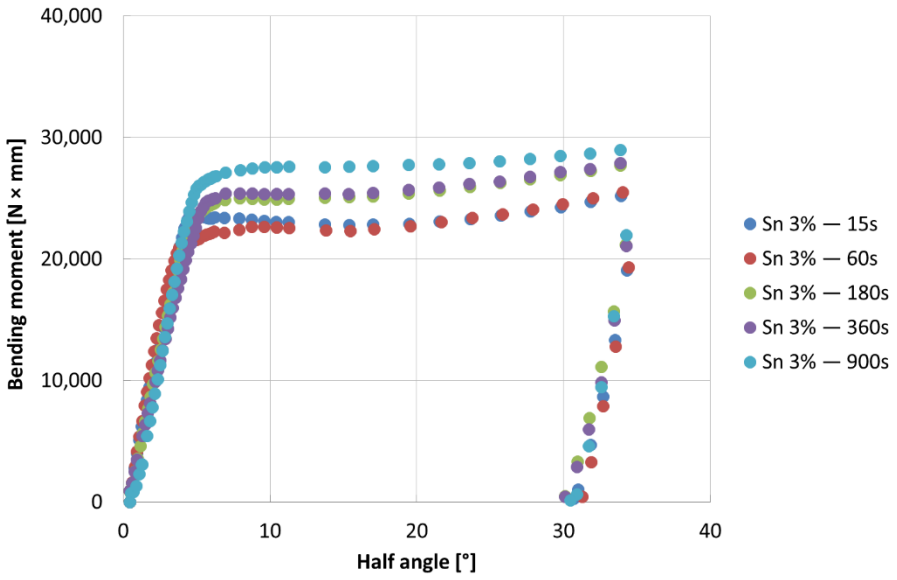

(**a**)

Figure 4. *Cont.*

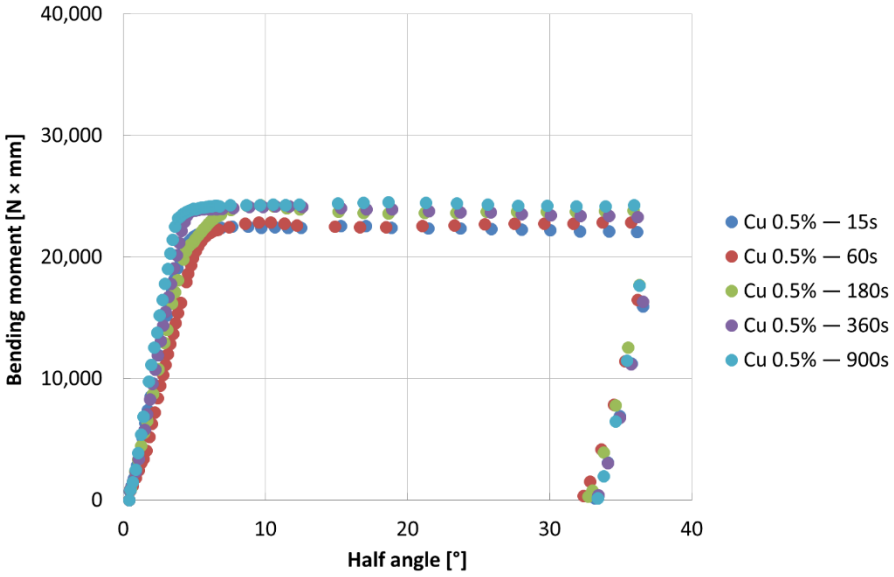

(**b**)

Figure 4. Bending tests results for specimens from: (**a**) Zn-Sn 3% bath, (**b**) Zn-Cu 0.5% bath.

The production processes of titanium-containing coatings have not yet been optimized so they are not present at an industrial level. Coatings that are able to change the surface colour, thanks to the control of the surface oxidation state at high temperatures, are generated by titanium addition in the zinc bath. Moreover, this element strongly influences the kinetics of the intermetallic phases formation and leads to quite high bending strength values, as shown in Figure 5.

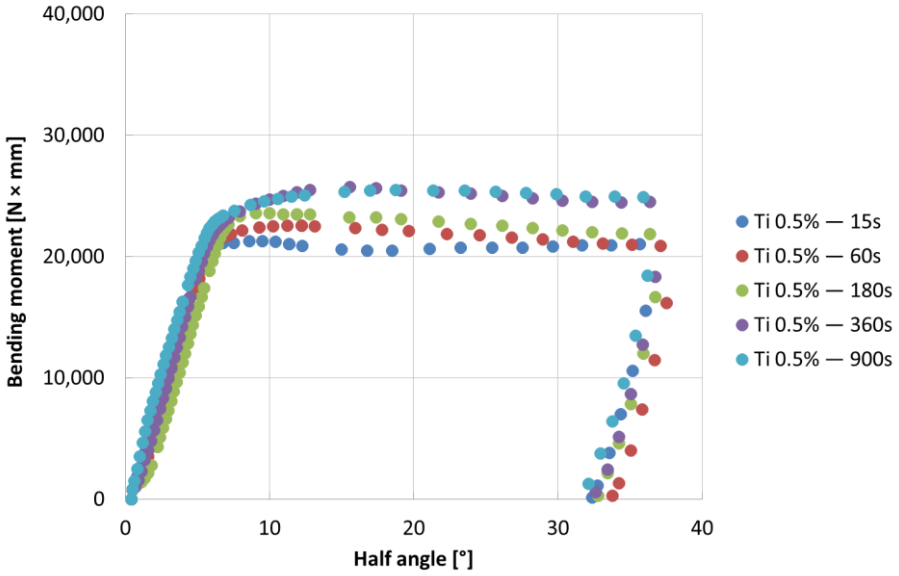

Figure 5. Bending tests results for specimens from Zn-Ti 0.5% bath.

The presence of aluminium in the galvanizing bath considerably lowers the kinetics of formation of the intermetallic phases. The thicknesses of the coatings obtained with the same immersion time are lower than all the coatings investigated in this work. The bending strength is also the lowest, as shown in the curves in Figure 6.

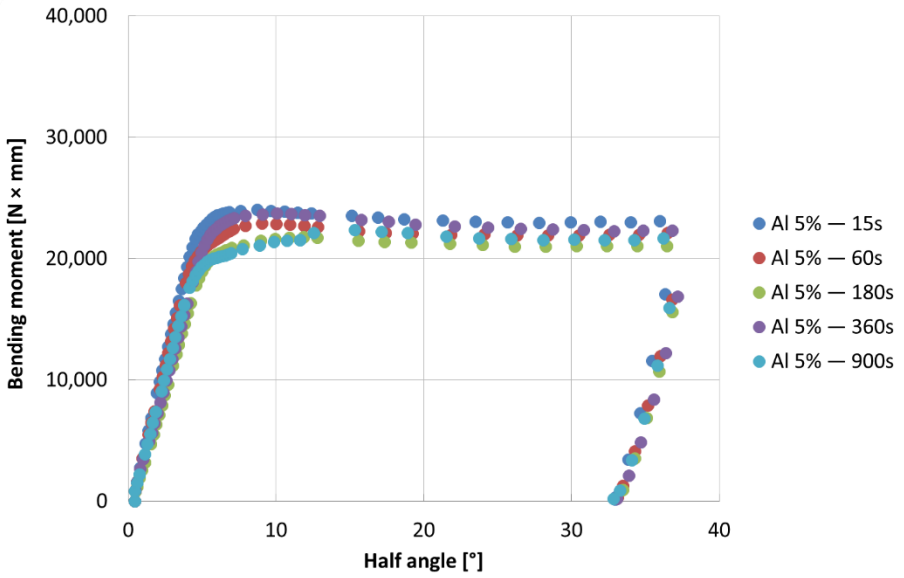

Figure 6. Bending tests results for specimens from Zn-Al 5% bath.

After 15 s of immersion, the bending test results for all five coatings are shown in Figure 7. As can be observed, the greatest bending moment of the Zn-Sn 3% coating is at the maximum loading angle (30°). The same is true for the bending findings after 900 s of coating immersion, as shown in Figure 8, where the maximum bending moment is that of Zn-Sn 3%.

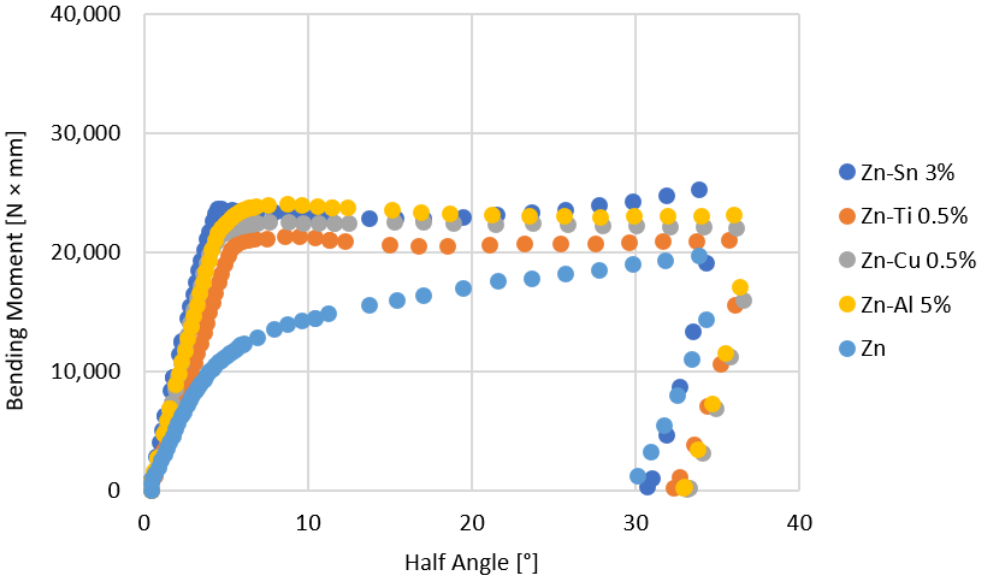

Figure 7. Bending tests results for all specimens investigated for 15 s dipping time.

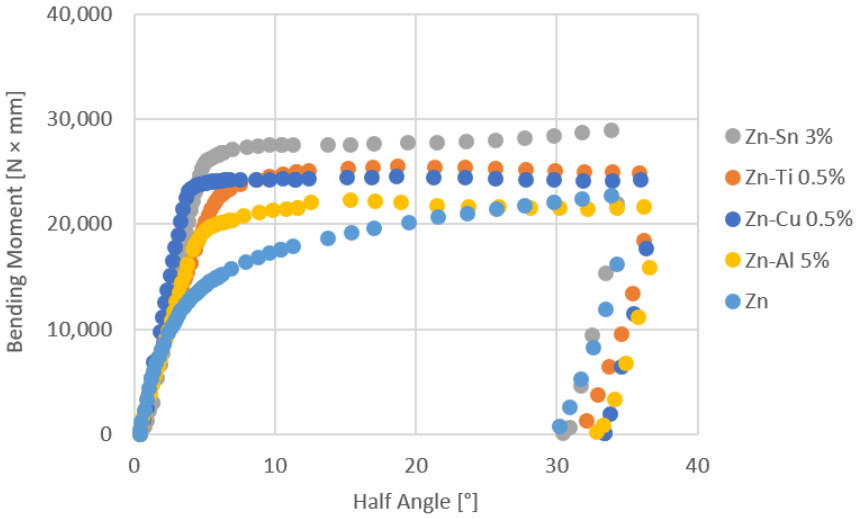

Figure 8. Bending tests results for all specimens investigated for 900 s dipping time.

Considering the coatings obtained from pure zinc baths and baths containing tin and copper, the LOM analysis showed the existence of the same intermetallic phases shown in Figure 1 and characterized by different thickness values. In particular, as shown in Figure 9, the following phases were observed:

- The phase δ is the closest one to the surface of the steel specimen in all specimens, except for Figure 9c were a poorly visible Γ phase is also present. The metallography of Figure 9c shows that δ phase is affected by radial cracks as a result of the variable thermal expansion during cooling, but there are other radial cracks due to the bending tests also in the baths containing tin and copper. All the cracks present in δ go through the phase, propagating in the ζ phase or stopping at the δ-ζ interface.
- The ζ phases are all with a well-developed columnar morphology, in all specimens, even those obtained at high immersion times. Radial cracks are also present in this phase, but they all come from the δ phase. These cracks go through the ζ phase or stop at the ζ-η interface. For this reason, the ζ phase is less fragile than the δ phase.
- Outside, the η phase can be observed in all images, which is even more ductile than the ζ phase as it is not crossed by any crack, as well explained by other authors [1].

The addition of 0.5% by weight of titanium determines a higher reactivity of the zinc bath on the substrate surface and the thicknesses obtained are greater, with the same immersion time, compared to all the cases investigated in this work. The coatings obtained from this bath have different intermetallic phases from those obtained from pure zinc baths or baths with the addition of tin or copper. In Figure 10 it can be observed that, due to the high reactivity of the bath, there is not only the production of a thick iron-rich phase, but also a matrix with a compact and ductile phase that is present alongside a lamellar phase [23].

In addition, a morphologically compact τ phase rich in iron and titanium is formed, and it is present in the matrix of the coating. In fact, thanks to the enrichment in titanium, this phase originates from the δ one and separates from it, moving into the compact matrix to create various layers. This phenomenon happens especially at long immersion durations. If the phase reaches the coating surface, it can spread in the bath at the outermost regions. On the other hand, titanium can originate the compact matrix and produce the lamellar phase inside the components. The great hardness of the τ phase is its primary characteristic.

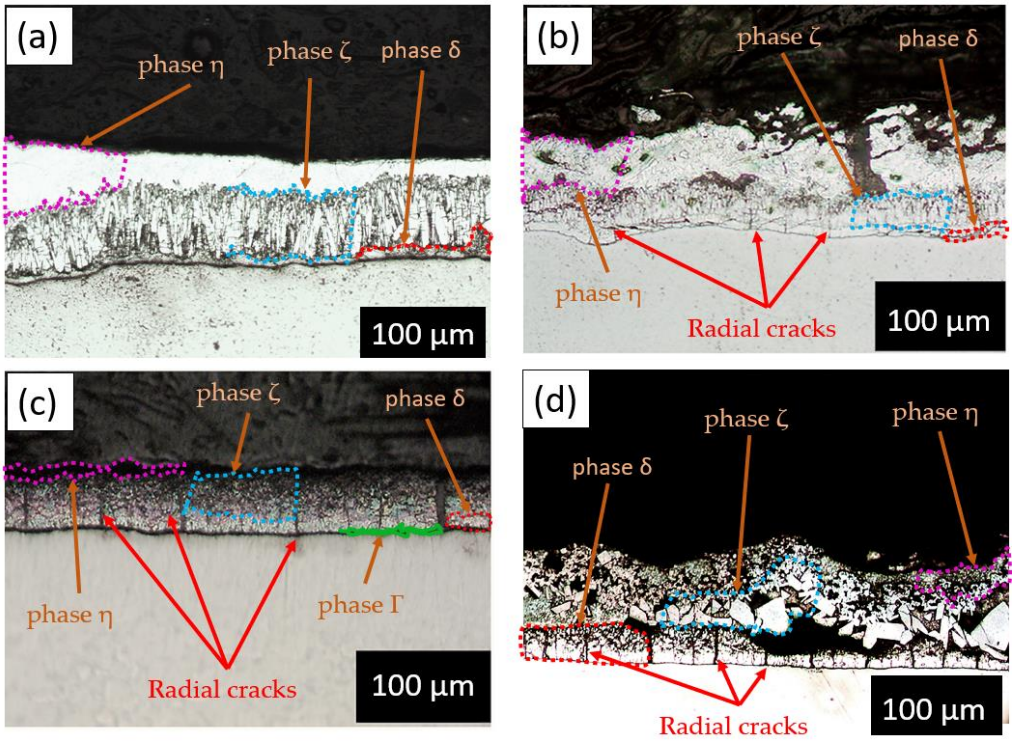

Figure 9. Metallographic analyses of coatings sections for: (**a**) Pure Zn—60 s; (**b**) Zn-Sn3%—60 s; (**c**) Z-Cu0.5%—60 s; (**d**) Zn-Ti 0.5%—60 s.

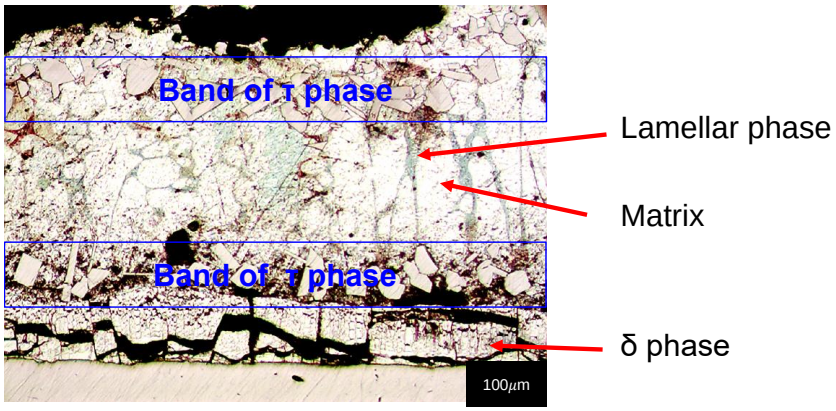

Figure 10. Coating microstructure from Zn-Ti 0.5% bath.

In bent specimen sections, longitudinal cracks in the δ phases are sometimes observed as well as the presence of intergranular cracks of τ phases, sometimes degenerating into a loss of τ grains. These kinds of damage cannot be taken into account in the adopted definition of damage (number of radial cracks for a millimetre of deformed arc length).

Baths containing 5% aluminium strongly reduce the kinetics of the formation of the intermetallic phases. The coatings obtained, after the immersion time, are characterized by the lowest thicknesses. The mechanism of formation of the coatings is different from those obtained by diffusion in the other baths. The presence of aluminium determines the formation of a parent phase of the coating characterized by high brittleness and a small thickness. This phase shatters near the surface and releases iron to the surrounding bath by diffusion, forming a "eutectic" type phase with a lamellar morphology that hinders the subsequent formation of the hard parent phase of the coating. As can be seen from the metallography in Figure 11, the coating is made up of the lamellar phase, with lamellae oriented in different ways.

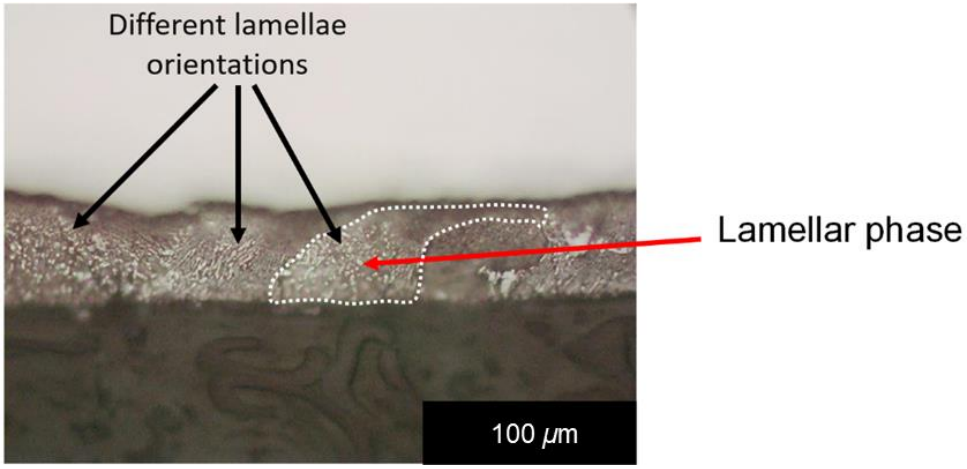

Figure 11. Microstructure of coatings obtained from Zn-Al 5%.

There are no radial cracks, so the coatings obtained are characterized by high ductility values.

In all the cases studied, except for the coatings obtained from baths containing aluminium, the main damage cause is the formation and propagation of radial cracks in the δ phase on the side subjected to tension. Therefore, the damage parameter was decided to be the number of radial cracks per deformed arc length. It can be shown in Figure 12 how the bending damage significantly rises in the case of coatings formed by pure Zn baths, by comparing the damages observed in the coatings produced through 180 s of immersion time for each tested bath. The effect of tin, on the other hand, increases the ductility of the coatings as there are lower damage values. Moreover, the presence of tin in the bath attenuates the increase in damage at elevated bending angles, enhancing the coating ductility.

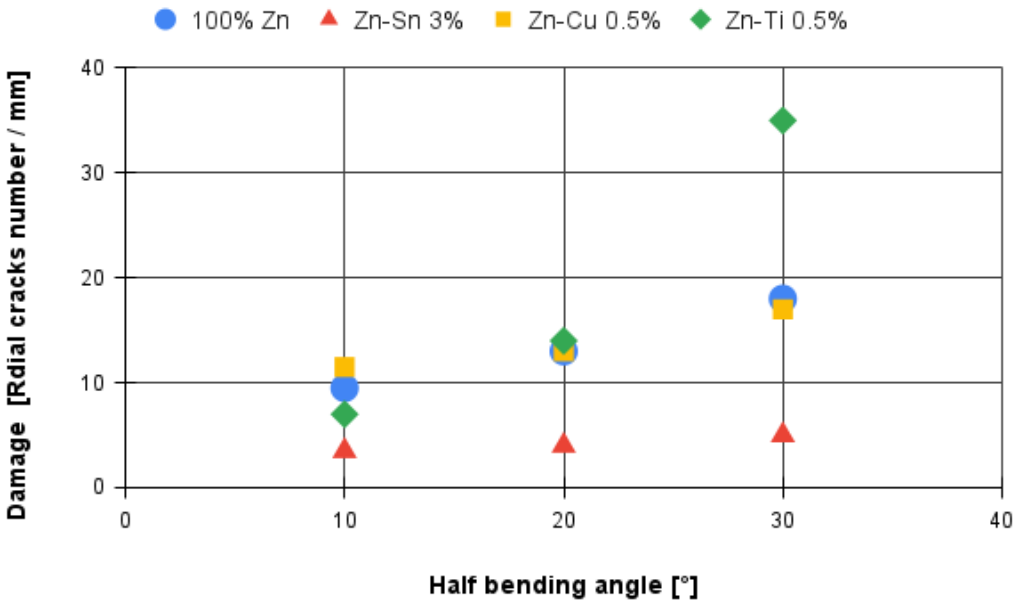

Figure 12. Damage of coatings produced with 180s of dipping time.

The effect of copper increases the damage values, and the behaviour is similar to the behaviour of coatings achieved from pure Zn bath. Considering the Ti-containing coatings, an increase in damage at an elevated strain value, comparable to the damage detected in pure Zn coatings, can be observed, but the values of the damage are the highest

among those investigated. The presence of titanium strongly increases the brittleness of the coatings.

4. Conclusions

In this study, galvanized coatings were produced using five distinct bath chemical compositions. In particular, pure zinc baths were considered, with the addition of 3% tin, 0.5% copper, 0.5% titanium and 5% aluminium. To investigate the kinetics of coating formation, several time periods were used. The dipping times investigated were 15, 60, 180, 360 and 900 s. The specimens were tested with a non-standardized bending tests (pure bending moment) and the coatings sections were studied by using a LOM to assess the occurrence of cracks and their propagation. In the case of hot dip galvanized thin plates, the non-standardized bending mechanism confirms its advantages over standardized three—or four-point bending tests, allowing bending tests to be performed in noncontact conditions and obtaining a pure constant bending moment for the entire specimen length. The damage parameter was defined as the number of radial cracks per millimetre of deformed arc. The observations were made on the tense part of the specimens subjected to bending at three different angles. The results can be outlined as follows:

- The production of the coating phases is significantly influenced by the chemical composition of the galvanizing bath, where in addition to the iron-rich phase, a new phase rich in iron and titanium is formed.
- The bending tests demonstrate that the phases mostly affect the specimens' resistance at high deformation levels; the higher bending moment values are due to the thickness of the coatings, which can be observed for longer immersion times (immersion time correlates with greater thickness, as well reported in the literature [24])
- For all the investigated coating conditions, radial cracks are observed. In conventional coatings, the cracks are originated at the substrate-coating interface, then they grow through the δ phase, and finally they stop in the ζ phase or at the δ-ζ interface, which demonstrate that δ is a brittle phase as well reported in literature [25].
- In the coatings characterized by the addition of Ti, the δ phase is characterized by the presence of radial cracks. Sometimes, delaminations may arise between the δ phase and the three-phase zone, while the τ phase is characterized by intergranular cracks.
- The coatings obtained from a bath with 5% aluminium never present radial cracks as well as the η phases in all investigated conditions. In addition, the thickness of the coating is very thin when compared with other coatings.

Radial cracks are prevalent in all coatings except aluminium, as demonstrated. The lack of cracks in this coating, as well as the fact that the thickness was significantly smaller at the same immersion periods, require additional investigation. It would be interesting to further examine the effect of aluminium at such high percentages in future studies (higher than the percentages used in industry). Furthermore, the addition of titanium to the zinc-aluminium bath should be tested with the objective of enhancing titanium ductility while preserving the natural colours that titanium offers at various degrees of oxidation [24].

Author Contributions: Conceptualization, all the authors; methodology, C.B. and V.D.C.; investigation, L.P.M. and F.I.; writing—original draft preparation, V.D.C. and L.P.M.; writing—review and editing, C.B. and F.I. All authors have read and agreed to the published version of the manuscript.

Funding: This research received no external funding.

Data Availability Statement: The data presented in this study are available on request from the corresponding author. The data are not publicly available due to privacy reasons.

Conflicts of Interest: The authors declare no conflict of interest.

References

1. Marder, A.R. The metallurgy of zinc-coated steel. *Prog. Mater. Sci.* **2000**, *45*, 191–271. [CrossRef]
2. Shibli, S.M.A.; Meena, B.N.; Remya, R. A review on recent approaches in the field of hot dip zinc galvanizing process. *Surf. Coat. Technol.* **2015**, *262*, 210–215. [CrossRef]
3. Proskurkin, E.V.; Gorbunov, N.S. *Diffusion Zinc Coatings*; Metallurgiya Press: Moscow, Russia, 1972.
4. Mackowiak, J.; Short, N.R. Metallurgy of galvanized coatings. *Int. Mater. Rev.* **1979**, *1*, 1–19. [CrossRef]
5. Tzimas, E.; Papadimitriou, G. Cracking mechanisms in high temperature hot-dip galvanized coatings. *Surf. Coat. Technol.* **2001**, *145*, 176–185. [CrossRef]
6. Natali, S.; Iacoviello, F.; Di Cocco, V. Damaging micromechanisms in hot-dip galvanizing Zn based coatings. *Theor. Appl. Fract. Mech.* **2014**, *70*, 91–98. [CrossRef]
7. Massalski, T.B.; Okamoto, H.L.; Subramanian, P.R.; Kacprzak, L. *Binary Alloy Phase Diagrams*, 2nd ed.; ASM International: Materials Park, OH, USA, 1996.
8. Carpinteri, A.; Di Cocco, V.; Fortese, G.; Iacoviello, F.; Natali, S.; Ronchei, C.; Scorza, D.; Vantadori, S. Kinetics of Intermetallic Phases and Mechanical Behavior of ZnSn3% Hot-Dip Galvanization Coatings. *Adv. Eng. Mater.* **2016**, *12*, 2088–2094. [CrossRef]
9. Vantadori, S.; Carpinteri, A.; Di Cocco, V.; Fortese, G.; Iacoviello, F.; Natali, S.; Ronchei, C.; Scorza, D.; Zanichelli, A. Novel zinc-based alloys used to improve the corrosion protection of metallic substrates. *Eng. Fail. Anal.* **2017**, *82*, 327–339. [CrossRef]
10. Nairin, J.A.; Kim, S.R. A fracture mechanics analysis of multiple cracking in coatings. *Eng. Fract. Mech.* **1992**, *42*, 195–208. [CrossRef]
11. Kim, S.R.; Narin, J.A. Fracture mechanics analysis of coating/substrate systems: Part I: Analysis of tensile and bending experiments. *Eng. Fract. Mech.* **2000**, *65*, 573–593. [CrossRef]
12. Vantadori, S.; Zanichelli, A.; Ronchei, C.; Scorza, D.; Di Cocco, V.; Iacoviello, F. Numerical Simulation of Traditional and Technological Zinc-Based Coatings: Part I. *Adv. Eng. Mater.* **2022**, *24*, 2101619. [CrossRef]
13. Al-Negheimish, A.; Hussain, R.R.; Alhozaimy, A.; Singh, D.D.N. Corrosion performance of hot-dip galvanized zinc-aluminum coated steel rebars in comparison to the conventional pure zinc coated rebars in concrete environment. *Constr. Build. Mater.* **2021**, *274*, 121921. [CrossRef]
14. Lin, K.L.; Chue, C.H.; Ching Kou, B. Deformation and corrosion of hot dip galvanized coatings. *Mater. Chem. Phys.* **1997**, *50*, 82–87. [CrossRef]
15. Di Cocco, V. Sn and Ti influences on intermetallic phases damage in hot dip galvanizing. *Fract. Struct. Integr.* **2012**, *22*, 31–38. [CrossRef]
16. Duncan, J.L.; Ding, S.C.; Jiang, V.L. Moment-curvature measurement in thin sheet—Part I: Equipment. *Int. J. Mech. Sci.* **1999**, *41*, 249–260. [CrossRef]
17. Lu, X. Correlation between Microstructural Evolution and Mechanical Properties of 2000 MPa Cold-Drawn Pearlitic Steel Wires during Galvanizing Simulated Annealing. *Metals* **2019**, *9*, 326. [CrossRef]
18. García-Martino, Á.; García, C.; Prieto, M.M.; Díaz, J. Prediction of Mechanical Properties for High Strength Low Alloyed Steels in a Commercial Hot Dip Galvanizing Line without Soaking Section. *Metals* **2020**, *10*, 561. [CrossRef]
19. Colla, V.; Cateni, S.; Maddaloni, A.; Vignali, A. A Modular Machine-Learning-Based Approach to Improve Tensile Properties Uniformity Along Hot Dip Galvanized Steel Strips for Automotive Applications. *Metals* **2020**, *10*, 923. [CrossRef]
20. Giorgi, M.L.; Guillot, J.B.; Nicolle, R. Theoretical model of the interfacial reactions between solid iron and liquid zinc-aluminium alloy. *J. Mater. Sci.* **2005**, *40*, 2263–2268. [CrossRef]
21. Min, T.; Gao, Y.; Huang, X.; Gong, Z.; Li, K.; Ma, S. Effects of aluminum concentration on the formation of inhibition layer during hot-dip galvanizing. *Int. J. Heat Mass Tran.* **2018**, *127*, 394–402. [CrossRef]
22. Di Cocco, V.; Iacoviello, F.; D'Agostino, L.; Natali, S. Damage micromechanisms in a hot dip galvanized steel. *Proc. Struct. Integr.* **2017**, *3*, 231–236. [CrossRef]
23. Sjoukes, F. Chemical reactions in fluxes for hot dip galvanizing. *Anti-Corros. Methods Mater.* **1990**, *37*, 12–14. [CrossRef]
24. Salles, P.; Pinto, D.; Hantanasirisakul, K.; Maleski, K.; Shuck, C.E.; Gogotsi, Y. Electrochromic effect in titanium carbide MXene thin films produced by dip-coating. *Adv. Funct. Mater.* **2019**, *29*, 1809223. [CrossRef]
25. Manna, M.; Naidu, G.; Rani, N.; Bandyopadhyay, N. Characterisation of coating on rebar surface using hot-dip Zn and Zn-4.9 Al-0.1 misch metal bath. *Surf. Coat. Technol.* **2008**, *202*, 1510–1516. [CrossRef]